Radial Basis Function Identifier and Pole-Shifting Controller for Power System Stabilizer Application

G. Ramakrishna, *Member, IEEE,* and O. P. Malik, *Life Fellow, IEEE*

***Abstract*—Use of a mixed structure consisting of a radial basis function (RBF) network and pole-shifting feedback controller for power system stabilizer application is presented in this paper. The RBF network is used to identify the time-varying parameters of the power system. The RBF has a simple structure with a nonlinear hidden layer which constructs local approximations to nonlinear input-output mapping and a linear output layer. The network is capable of fast learning and represents a nonlinear autoregressive moving average model with exogeneous inputs (NARMAX). The NARMAX model is transformed into a linear ARMA model every sampling period and the pole-shift controller is used to calculate the control signal. This process of linearizing a nonlinear system is important because of the widespread industrial acceptance of linear feedback controllers, availability of theoretical and practical results about robustness, and closed-loop stability. Simulation studies carried out on a single-machine infinite bus power system verify the effectiveness of the above approach.**

***Index Terms*—ARMA model, pole-shift control, power system stabilizer, radial basis function network.**

I. Introduction

THE Conventional PSS (CPSS) is widely used in today's excitation controls [1]. It is designed for a particular operating condition around which the transfer function of a linearized model of the system is obtained. Usually the operating condition where generator operates most of the time is chosen [2]. The CPSS designed for one operating condition generally cannot maintain the same quality of performance at other operating points [3]. In addition, the parameters of the CPSS need to be re-tuned when applied to a new generating unit or when the network configuration changes.

An adaptive PSS (APSS) provides a possible way to solve the above mentioned problem relating to the CPSS [4]. Self-tuning (or indirect adaptive control) based APSS is one of the popular adaptive control techniques reported in the literature [5].

The work on adaptive control techniques has highlighted two main points.

- Firstly, the techniques such as self-tuning regulators, pole assignment (PA) methods, are generally developed assuming that a low-order discrete model is a close approximation to the power system [3], [6], [7]. However, since the power system is a high-order nonlinear continuous system, it is hard for the low-order discrete model to precisely describe the dynamic behavior of the power system. Consequently, a high-order model is used to represent the power system, which requires a significant amount of computation. This in turn limits the control effect, as the system is unable to act at higher sampling rates.
- Secondly, the control strategy should be robust and stable for industrial use.

Neural networks (NNs) transform the inputs in a low-dimensional space to high-dimensional nonlinear hidden unit space and hence are more likely to model the nonlinear characteristics of the power system. Furthermore, the ability of NNs to learn makes it attractive for use in adaptive control techniques [8]. Starting with an off-line trained NN, it requires small computation time to update the weights on-line and thus track the system operating conditions. This feature makes it a good candidate for modeling in a real-time controller. Applications of NNs for power system control and identification have been reported in various publications [9]–[11]. Among all the applications, PSS has been the most popular application area [12].

A neural network identifier to track and identify the nonlinear plant in real-time and a neuro-controller to damp power system oscillations is described in [12]. While such neuro-adaptive PSSs are effective in damping mechanical oscillations, there are unresolved issues relating to their practical use. In particular, stability and robustness cannot be proven numerically for the neuro-controller. To overcome the above difficulty, an adaptive controller consisting of a RBF network identifier and the numerically stable PS feedback control system is proposed in this paper.

The paper is organized as follows: The controller structure is described in Section II. The RBF identifier is explained in Section III and a brief description of the PS control algorithm is given in Section IV. Simulation results with the controller as a PSS are given in Section V.

II. Controller Architecture

The RBF network is used for identification. RBF maps the low-order input space consisting of past samples of the output and the control signal into a high-dimensional nonlinear space in the hidden layer consisting of Gaussian functions. The outputs from the hidden layer are weighted and connected to a linear output layer. The linear characteristic of the output layer means that linear filtering algorithms can be applied for adjusting the weights and can be updated rapidly [13]. Once RBF is trained to represent the nonlinear model of the power system, the RBF

Manuscript received January 16, 2002; revised June 18, 2003. Paper no. TEC-00072-2002.

G. Ramakrishna is with the Department of Electrical Engineering, University of Saskatchewan, Saskatoon, SK S7N 5A9, Canada (e-mail: rama.krishna@usask.ca).

O. P. Malik is with the Department of Electrical and Computer Engineering, The University of Calgary, Calgary, AB T2N 1N4, Canada (e-mail: malik@enel.ucalgary.ca).

Digital Object Identifier 10.1109/TEC.2004.837268

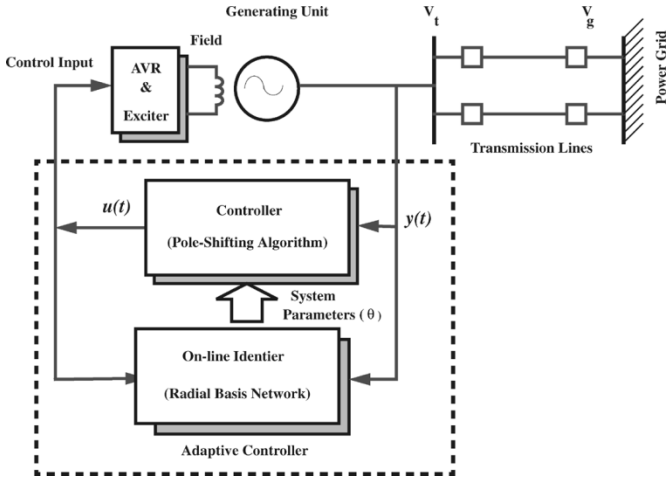

Fig. 1. Power system with adaptive controller as PSS.

is combined with a PS controller [14] to stabilize the output. The nonlinear relationships between the input and output of RBF (NARMAX model) are linearized every sampling period to obtain an ARMA relationship for use in the pole-shifting controller. The unstable poles are moved inside the unit circle in the z-plane and the control calculated so as to achieve regulation of the system to the constant setpoint in the shortest period of time.

Structure of the adaptive controller as a PSS is shown in Fig. 1. The adaptive PSS (APSS) consists of an RBF identifier and a pole-shifting controller. In the proposed APSS, the generating unit is identified by a third order discrete ARMA model [14].

$$A(z^{-1})y(t) = B(z^{-1})u(t) + d(t) \tag{1}$$

$$A(z^{-1}) = 1 + a_1 z^{-1} + a_2 z^{-2} + a_3 z^{-3} \tag{2}$$

$$B(z^{-1}) = b_1 z^{-1} + b_2 z^{-2} + b_3 z^{-3}. \tag{3}$$

The variables $y(t)$, $u(t)$ and $d(t)$ are the system output, system input and white noise respectively. Equation (1) is rewritten in a form suitable for identification as

$$y(t) = \theta^T(t)\Psi(t) + d(t) \tag{4}$$

where

$$\theta(t) = [a_1\ a_2\ a_3\ b_1\ b_2\ b_3] \tag{5}$$

is the parameter vector (regression coefficients) and (6), shown at the bottom of the page, is the measurement variable vector.

III. RBF Network Identification

The RBF model [13] shown in Fig. 2 is used to identify the ARMA parameters given in (5). It consists of two layers: a hidden layer consisting of radially symmetric basis functions and a linear output layer. The hidden layer nodes consist of a

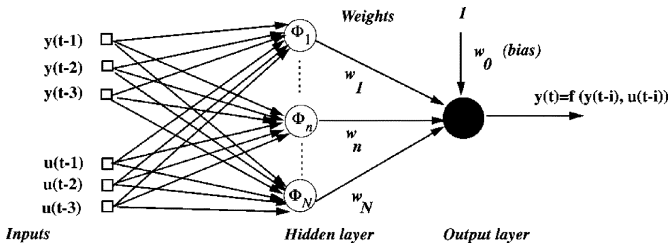

Fig. 2. Radial basis function network model.

parameter vector called centers. Each node calculates the Euclidean distance between the center and the network input vector and the result is passed through a Gaussian function

$$\phi(x) = e^{-x^2/\sigma^2}. \tag{7}$$

The overall input-output response of the RBF network is given by

$$y = w_o + \sum_{n=1}^{N} w_n \exp\left(-\frac{\|x_p - c_n\|^2}{\sigma^2}\right). \tag{8}$$

In (7) and (8), x_p is the input vector, w_o is the biasing term, w_n is the weight between the hidden nodes and the output, c_n is the center of the hidden node, σ is the width of the hidden node, N the number of hidden nodes and $\phi(.)$ denotes the Gaussian function.

The topology of the RBF network is very similar to the two layer perceptrons [13], the main difference being the characteristics of the hidden nodes. It is shown in [15] that any continuous function can be uniformly approximated to an arbitrary accuracy by an RBF network and it is shown in [16] that RBF exhibits the best approximation property confirming the importance of this architecture.

Many algorithms are available for training the RBF (finding RBF centers and weights) [13], [17]. For on-line identification using RBF, it has been also found that updating of RBF centers and weights improves both the modeling capability and the tracking property [17].

In this work, the learning algorithm described in [18] is used for updating the centers and weights simultaneously during both off-line training and on-line updating. The RBF hidden nodes are created one at a time. The following steps are repeated until the network's mean squared error is minimized.

1) The input vector with the greatest error is found after each cycle of presentation.
2) A hidden node is added with center equal to that vector.
3) The linear weights are redesigned using Widrow–Hoff **[18]** learning algorithm. Steps 1–3 are repeated until the error is minimized.

The Widrow–Hoff learning algorithm [18] for calculations of weights is summarized below:

$$\Psi(t) = [-y(t-1) \quad -y(t-2) \quad -y(t-3) \quad u(t-1) \quad u(t-2) \quad u(t-3)]^T \tag{6}$$

- The weight equations

$$\mathbf{W}(n+1) = \mathbf{W}(n) + 2\alpha e(n)\mathbf{x}^T(n)$$
$$w_0(n+1) = w_0(n) + 2\alpha e(n) \tag{9}$$

where α is the learning rate.

The learning rate, α, decide the speed of convergence of the iterative procedure. If α is large, learning occurs quickly, but if it is too large it leads to instability and the errors may even increase. To ensure stable learning, the learning rate is chosen as less than the reciprocal of the largest eigenvector of the correlation matrix of $\mathbf{x}^T\mathbf{x}$ [18].

- The output error criterion (mean-squared error (MSE) performance index) is given by the following equations:

$$MSE = \frac{1}{N}\sum_{n=1}^{N} e(n)^2 = \frac{1}{N}\sum_{n=1}^{N}(y(t) - \hat{y(t)})^2. \tag{10}$$

The RBF represents a NARMAX model [17]. To obtain the linear parameters (cf. (5)) of the standard ARMA model, the output of the RBF, $y(t) = f(y(t-i), u(t-i))$, is linearized using the Taylor series expansion and retaining only the linear term

$$\Delta y = \frac{\partial y}{\partial y(t-1)}\Delta y(t-1) + \cdots + \frac{\partial y}{\partial u(t-1)}\Delta u(t-1) + \cdots. \tag{11}$$

The partial derivative terms, $[\partial y/\partial \mathbf{x}_i]$ are the elements of the RBF network Jacobian $[J_y]$ and are given by

$$\frac{\partial y}{\partial \mathbf{x}_i} = 2\frac{(\mathbf{c}_{i,n} - \mathbf{x}_i)}{\sigma_n}\exp\left(-\sum_{i=1}^{N}\left(\frac{\mathbf{x}_i - \mathbf{c}_{i,n}}{\sigma_n}\right)^2\right). \tag{12}$$

N represents the total number of hidden nodes. n is the node number.

The process of linearizing the NARMAX model of RBF is an important point, for by linearizing it is possible to apply linear analysis control methods such as the PS control technique to obtain the control signal. The PS control technique is described in Section IV.

For the studies described in this paper, the active power deviation (ΔP_e), of the generating unit is sampled at the rate of 20 Hz and is used as input to the stabilizer ($y = \Delta P_e$) (cf. Figs. 1 and 2). For off-line training of the RBF identifier, data was collected at selected operating conditions in the range of 0.3 *pu* to 1.1 *pu* power output and 0.7 *pf* lag to 0.9 *pf* lead. The disturbances used were input torque reference disturbances, voltage reference changes, and a three-phase to ground fault.

The off-line training yields 17 hidden nodes in the RBF network. After the off-line training, the network is further updated on-line during every sampling period making it an adaptive approach.

As the system undergoes only a small change if viewed under one sampling window (50 ms) during on-line identification and the error remains well below the MSE, the RBF centers do not add up during on-line identification. Only the linear weights governed by (9) are updated to achieve on-line tracking. This provides additional benefit as the size of the RBF remains within reasonable limits during on-line identification and the real-time calculation needs can be met.

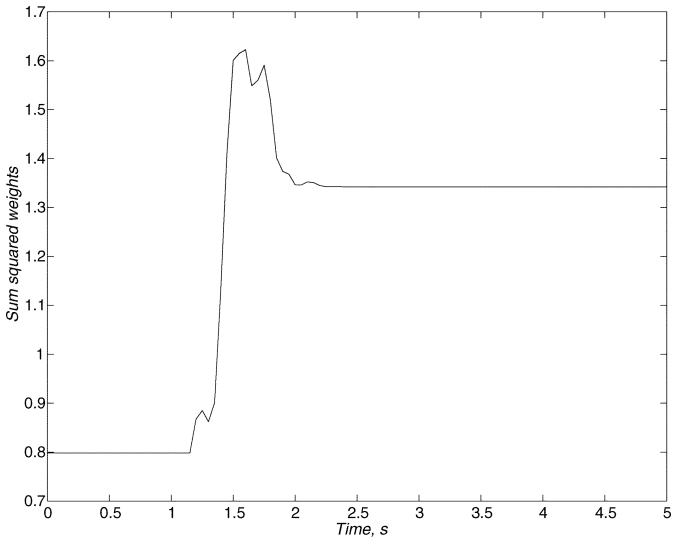

Fig. 3. Sum squared variation of RBF weights during a three-phase to ground fault.

The generating unit parameters when scaled into *pu* values fall under a narrow range and differ only slightly from one generating unit to another. Therefore, RBF-Identifier does not need off-line training for a new setup. Instead, the off-line values of centers and weights of the RBF-Identifiers can be directly adopted for a new generating unit. This is favorable from the practical point-of-view as it alleviates the need for off-line training whenever the APSS is used on a new generating unit. Slight mis-matches that can occur when it is ported to a different unit is taken care of in the first few iterations of on-line adaptation. Such an advantage does not exist for a CPSS whose parameters have to be re-tuned whenever it is applied to a new unit.

Fig. 3 shows the variation of the sum of RBF linear weights squared, with on-line updating, during a three-phase to ground fault applied at 1.0 s at the middle of one transmission line. The fault is cleared 50 ms later by opening the breakers at both ends. The initial operating conditions are 0.7 *pu* active power delivered to the bus at 0.85 *pf* lag.

The RBF centers find local approximations to different portions of the input space. Thus the RBF is locally responsive to small disturbances and is suitable for incremental updating of the weights without losing generalization capability. Thus the RBF is easier to train than feed-forward NNs which use global generalization. Another advantage of RBF is its simpler topology over feed-forward NNs which may require more than one hidden layer. Consequently, designing the RBF is faster and it is capable of faster learning than feed-forward networks. Moreover, when the NNs are used to solve the nonlinear regression problems, a linear output layer is desirable and hence the RBF is the preferred choice.

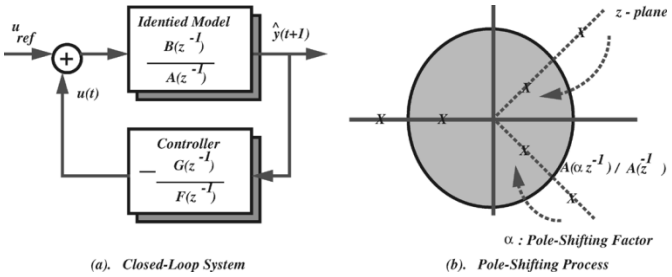

Fig. 4. Closed-loop system block diagram and the pole-shifting (PS) process.

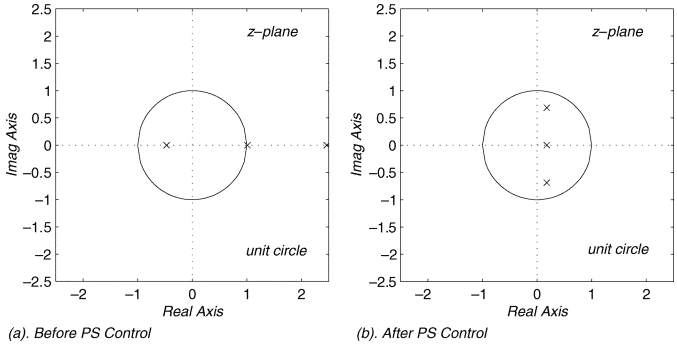

Fig. 5. Stability test for the PS control: pole-pattern for $T(z^{-1})$.

IV. Adaptive Pole-Shifting (PS) Controller

Once the system model is identified as in (1), the control signal can be calculated based on this model. In this paper, the self-optimizing PS control algorithm described in [14] is employed to generate the control signal. The PS process is briefly described next.

For the system modeled by (1), assume that the feedback loop has the form [cf. Fig. 4(a)]

$$\frac{u(t)}{y(t)} = -\frac{G(z^{-1})}{F(z^{-1})}. \tag{13}$$

From (1) and (13) the closed-loop characteristic polynomial $T(z^{-1})$ can be derived as

$$A(z^{-1})F(z^{-1}) + B(z^{-1})G(z^{-1}) = T(z^{-1}). \tag{14}$$

Unlike the pole-assignment (PA) algorithm, in which $T(z^{-1})$ is prescribed [19], the PS control algorithm makes $T(z^{-1})$ take the form of $A(z^{-1})$ but the pole locations are shifted by a factor α, i.e.,

$$T(z^{-1}) = A(\alpha z^{-1}). \tag{15}$$

In the PS algorithm, α, a scalar, is the only parameter to be determined and its value reflects the stability of the closed-loop system. Supposing λ is the absolute value of the largest characteristic root of $A(z^{-1})$, then $\alpha.\lambda$ is the largest characteristic root of $T(z^{-1})$. To guarantee the stability of the closed-loop system, α ought to satisfy the following inequality (stability constraint):

$$-\frac{1}{\lambda} < \alpha < \frac{1}{\lambda}. \tag{16}$$

The PS process is presented schematically in Fig. 4(b). It can be seen that once $T(z^{-1})$ is specified, $F(z^{-1})$ and $G(z^{-1})$ can be determined by (14), and thus the control signal $u(t)$ can be calculated from (13).

To consider the time domain performance of the controlled system, a performance index J is formed to measure the difference between the predicted system output, $\hat{y}(t+1)$ and its reference, $y_r(t+1)$

$$J = E[\hat{y}(t+1) - y_r(t+1)]^2. \tag{17}$$

E is the expectation operator. $\hat{y}(t+1)$ is determined by system parameter polynomials $A(z^{-1})$, $B(z^{-1})$ and past $y(t)$ and $u(t)$ signal sequence. Considering that $u(t)$ is a function of the pole-shifting factor α, the performance index J becomes

$$\min_{\alpha} J = F[A(z^{-1}), B(z^{-1}), u(t), y(t), \alpha, y_r(t+1)]. \tag{18}$$

In (18) $F[.]$ denotes function. The pole-shifting factor α is the only unknown variable in (18) and thus can be determined by minimizing J.

Constraints

When minimizing $J(t+1, \alpha)$, it should be noted that α will be subject to the following constraints.

1) The stabilizer must keep the closed loop system stable. It implies that all roots of the closed-loop characteristic polynomial ($A(\alpha z^{-1})$) must lie within the unit circle in the z-plane [cf. (16)].
2) The control limit should be taken into account in the stabilizer design to avoid servo saturation or equipment damage. The optimal solution of α should also satisfy the following inequality (control constraint):

$$u_{\min} \le u(t, \alpha) \le u_{\max}. \tag{19}$$

The pole-patterns of $T(z^{-1})$ are shown in Fig. 5 for the three-phase fault described in Section III. Fig. 5(a) shows the pole-patterns before the application of control. Since two poles map outside the unit circle, the system is in an unstable state. Fig. 5(b) shows the pole-pattern after the PS control is applied. Since all the poles lie within the unit circle, the closed-loop system is stable. It shows that the PS control assures the stability of the closed-loop system and also optimizes the performance given by (18).

V. Simulation Results

Performance of the APSS with the proposed RBF identifier and the PS feedback control system is investigated on a synchronous generator connected to a constant voltage bus through two transmission lines (Fig. 1). A nonlinear seventh-order model is used to simulate the dynamic behavior of the single-machine infinite bus power system [20]. The differential equations used to simulate the synchronous generator and the parameters used in simulation studies are given in the Appendix [12]. An IEEE Standard 421.5, Type ST1A AVR

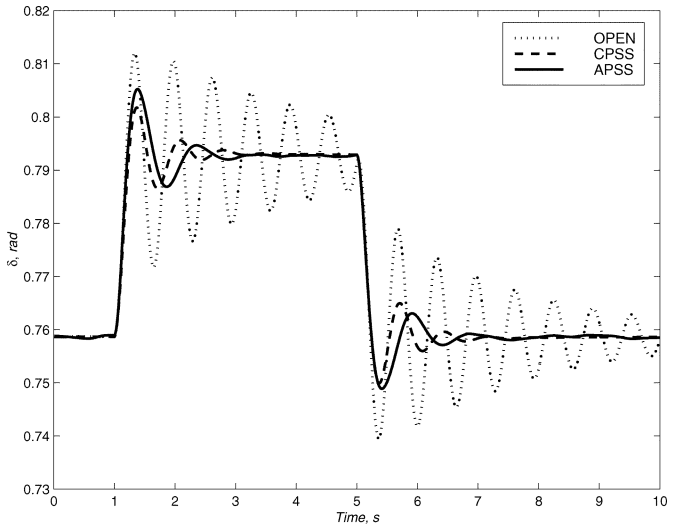

Fig. 6. Response to a 0.05 pu step increase in torque and return to initial conditions under peak load.

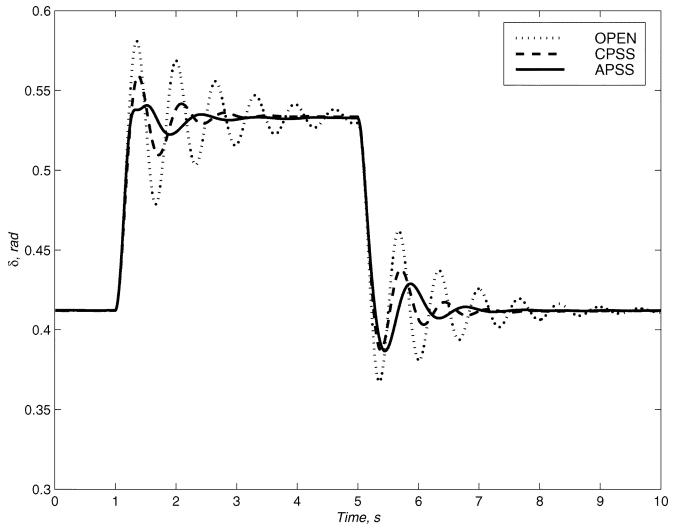

Fig. 7. A 0.15 pu change in torque and return to original condition in light load test.

and Exciter Model and an IEEE Standard 421.5, PSS1A Type CPSS [21] are used in simulation studies. The active power deviation, $\Delta P_e(k)$, is sampled at the rate of 20 *Hz* for parameter identification and control computation. Studies performed with various sampling rates show that the performance is practically the same for a sampling rate in the range of 20–100 *Hz*. Sampling frequencies above 100 *Hz* are of no practical benefit and the performance deteriorates for sampling rates under 20 *Hz*. A sampling rate of 20 *Hz* is chosen to make sure that there is enough time available for updating the RBF weights and control computation. ΔP_e is used as an input to the APSS instead of $\Delta\omega$ as it is readily available as an output signal in commercial AVRs. The control output is limited to 0.1 *pu*. The performance of the proposed APSS is shown under the following test conditions.

A. Peak Load Conditions

In this test, the generator is operating at 0.97 *pu* power, 0.97 *pf lag*, 1.075 *pu* terminal voltage. This gives a generator *VA* loading of 1.0 *pu*.

Under the above conditions, a 0.05 *pu* step increase in torque reference is applied at 1.0 *s* and then removed at 5.0 *s*. The CPSS parameters were tuned for 1.0 *pu VA* loading using the tuning procedure described in [22]. The parameters of the CPSS were then kept unchanged for all the tests described in this paper.

The power angle (δ) response of the APSS, CPSS and the open-loop (without stabilizer) are shown in Fig. 6. It can be seen from the figure that the performance of the two is very close.

B. Light Load Conditions

With the system operating under a light load condition of 0.5 *pu* power at 0.94 *pf lag*, 1.075 *pu* terminal voltage, a 0.15 *pu* step increase in input torque reference is applied. The disturbance is large enough to cause the system to operate in a nonlinear region. System response for these nonlinear conditions is shown in Fig. 7. The APSS shows the ability to adapt to a new operating condition and give good performance results.

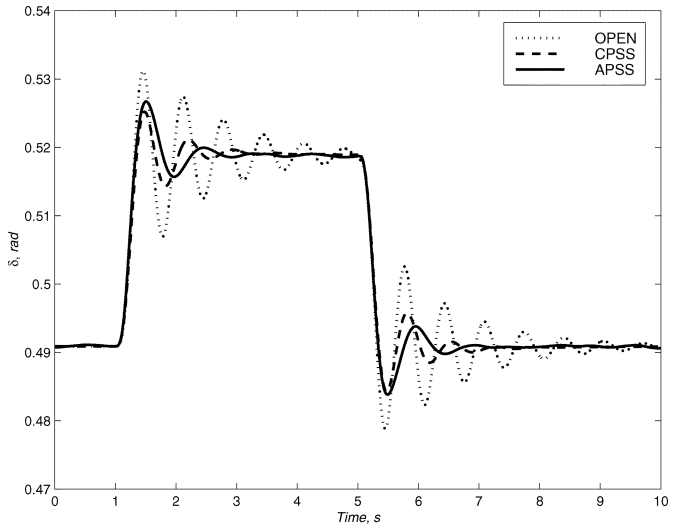

Fig. 8. Response to a 0.02 pu step decrease in reference voltage and return to initial condition.

C. Voltage Reference Change

In this test, the operating condition is 0.60 *pu* power and 0.95 *pf lag* and 1.075 *pu* terminal voltage. A 0.02 *pu* decrease in voltage reference is applied at 1.0 *s* and removed after 5 *s*. The results are shown in Fig. 8. In the open loop system without any PSS, the system oscillates before stabilizing to the steady-state value. This is because the system stability margin decreases as the reference voltage drops for a certain active power output. It can be seen from Fig. 8 that the oscillations are effectively damped by APSS for both reference voltage decrease and increase.

Fig. 9 shows the V_t response. The results show that the terminal voltage (V_t) response is not compromised by using a PSS (a difference at the third decimal place) as the stabilizers essentially focus on damping the power oscillations in the power system [cf. (17)].

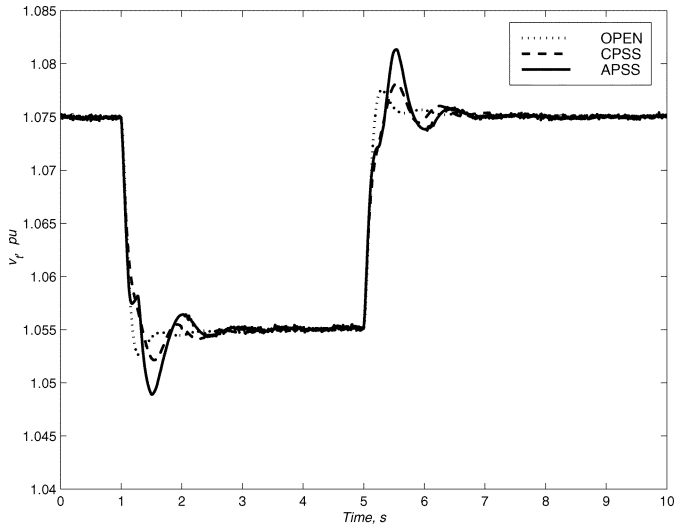

Fig. 9. V_t response for 0.02 pu voltage reference step change.

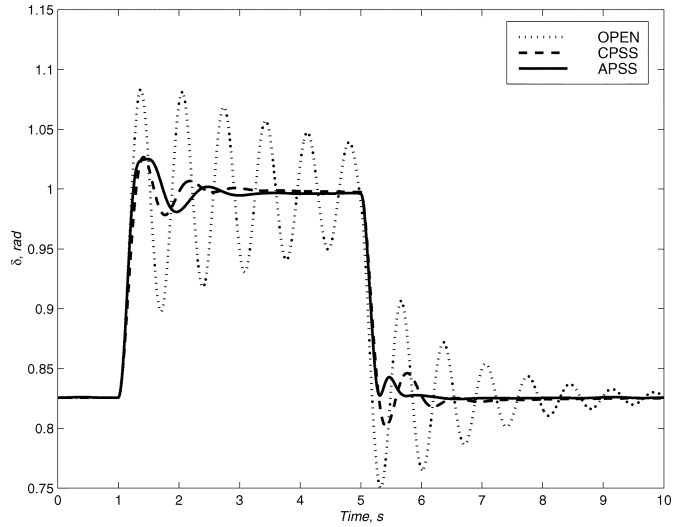

Fig. 10. Response to a 0.20 pu step increase in torque under leading power factor conditions.

D. Leading Power Factor Conditions

When the generator is operating at a leading power factor, it is a difficult situation for the controller because the stability margin is reduced. However, in order to absorb the capacitive charging current in a high voltage power system, it may become necessary to operate the generator at a leading power factor. It is, therefore, desirable that the controller be able to guarantee stable operation of the generator under leading power factor condition.

With the generator operating at a power of 0.7 *pu* with 0.96 *pf lead*, 0.95 *pu* terminal voltage a 0.2 *pu* step increase in torque reference was applied. The results given in Fig. 10 show that the oscillation of the system is damped out rapidly and demonstrates the effectiveness of the APSS to control generator under leading power factor operating conditions.

E. Fault Test

To verify the behavior of the APSS under transient conditions, a fault is applied to the system. The fault conditions are 0.5 *pu* power, 0.93 *pf* lag. The line is restored after 5.0 s by reclosing the circuit breakers at both ends.

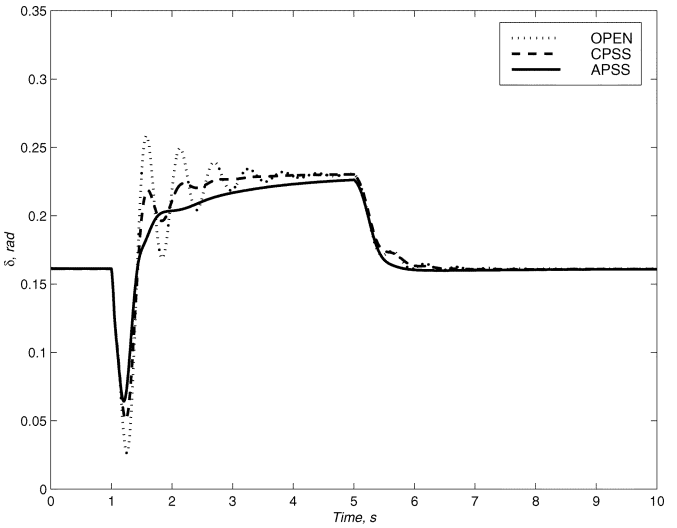

Fig. 11. System response to a three-phase to ground fault at the middle of one transmission line.

The results given in Fig. 11 show that APSS minimizes the deviation of power angle of the generator after the fault.

VI. Conclusions

Simulation results show that the proposed APSS has very good damping characteristics for different operating conditions and disturbances. The proposed APSS has the following advantages because of RBF modeling and PS feedback.

- The Gaussian functions in RBF provide local approximations. Hence the network is locally responsive to small disturbances and is suitable for incremental training of the weights without losing generalization capability. The feed-forward networks use global generalization and are less suitable for on-line updating of weights.
- The RBF stores "*a priori*" knowledge because of off-line training and can be updated with less computations. These properties make it attractive for real-time applications.
- The RBF-Identifier does not need off-line training for a new generating unit. This is favorable from practical point-of-view as it alleviates the need for off-line training whenever the APSS is used on a new generating unit. To remain fully effective, the parameters of a CPSS have to be re-tuned whenever it is applied to a new unit, or the system configuration changes.
- The RBF is a NARMAX model and hence is more suitable to represent the nonlinear nature of power systems. The NARMAX model is transformed into a linear model (ARMA) every sampling period for use in the PS controller. Thus a difficult nonlinear control problem is converted into an easier linear regression problem.
- The PS controller moves the unstable poles inside the unit circle in the z-plane and the control is calculated so as to optimize the output performance. The robustness and closed-loop stability condition would not be possible if a neuro-controller is used instead.

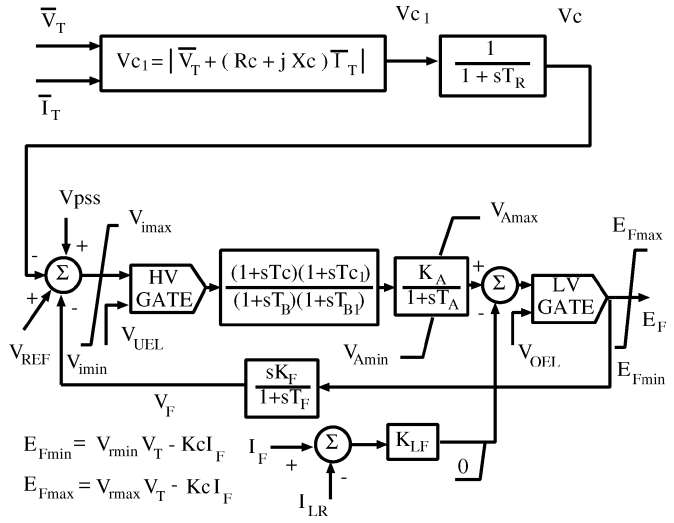

Fig. 12. AVR and exciter model.

The effectiveness of the RBF identifier based APSS in damping local and inter-area mode oscillations on a multi-machine power system was presented in [23]. Experimental results using the proposed APSS on a physical model of a power system have been documented in [24] and will be reported in detail shortly.

Appendix
System Model And Parameters

1) Generator

$$\begin{aligned}
\dot{\delta} &= \omega_0 \omega \\
\dot{\omega} &= \frac{\omega_0}{2H}(T_m + g + K_d\dot{\delta} - T_e) \\
\dot{\lambda}_d &= v_d + r_a i_d + \omega_o(\omega+1)\lambda_q \\
\dot{\lambda}_q &= v_q + r_a i_q - \omega_o(\omega+1)\lambda_d \\
\dot{\lambda}_f &= e_f - r_f i_f \\
\dot{\lambda}_{kd} &= -r_{kd} i_{kd} \\
\dot{\lambda}_{kq} &= -r_{kq} i_{kq} \\
\lambda_d &= (L_{md} + l_a) i_d + L_{md} i_{kd} + L_{md} i_f \\
\lambda_{kd} &= L_{md} i_d + L_{kd} i_{kd} + L_{md} i_f \\
\lambda_f &= L_{md} i_d + L_{md} i_{kd} + L_f i_f \\
\lambda_q &= (L_{mq} + l_a) i_d + L_{mq} i_{kq} \\
\lambda_{kq} &= L_{mq} i_q + L_{kq} i_{kq}.
\end{aligned}$$

2) Transmission network

$$\begin{aligned}
v_d &= v_b \sin\delta + r_e i_d - x_e i_q \\
v_q &= v_b \cos\delta + r_e i_q + x_e i_d.
\end{aligned}$$

3) IEEE standard type ST1A AVR and exciter model, Fig. 12.

4) Governor transfer function

$$g = \left[a + \frac{b}{1+sT_g}\right]\dot{\delta}.$$

5) IEEE standard PSS1A type conventional PSS, Fig. 13.

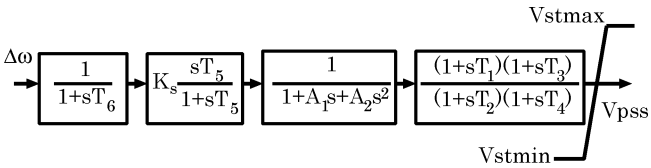

Fig. 13. IEEE standard PSS1A power system stabilizer.

6) Parameters used in the simulation studies

$$\begin{aligned}
r_a &= 0.007 \quad r_f = 0.000\,89 \quad r_{kq} = 0.023 \\
r_{kd} &= 0.023 \quad x_q = 0.743 \quad x_d = 1.24 \\
x_{md} &= 1.126 \quad x_{mq} = 0.626 \quad x_f = 1.33 \\
x_{kd} &= 1.1500 \quad x_{kq} = 0.652 \quad H = 3.46 \\
K_d &= -0.027 \quad r_t = 0.05 \quad x_t = 0.3 \\
R_C &= 0.0 \quad X_C = 0.0 \quad K_C = 0.08 \\
T_C &= 1.0 \quad T_B = 10.0 \quad T_{C1} = 0.0 \\
T_{B1} &= 0.0 \quad T_A = 0.0 \quad K_A = 190.0 \\
T_F &= 1.0 \quad K_F = 0.05 \quad T_R = 0.04 \\
V_{I\mathrm{MIN}} &= -999 \quad V_{I\mathrm{MAX}} = 999 \quad V_{A\mathrm{MAX}} = 999 \\
V_{A\mathrm{MIN}} &= -999 \quad V_{R\mathrm{MAX}} = 999 \quad V_{R\mathrm{MIN}} = -999 \\
V_{UEL} &= -999 \quad V_{OEL} = 999 \\
a &= -0.001\,33 \quad b = -0.17 \quad T_g = 0.25 \\
T_1 &= 0.10 \quad T_2 = 0.01 \quad T_3 = 0.10 \\
T_4 &= 0.01 \quad T_5 = 2.85 \quad T_6 = 0.005 \\
A_1 &= 0.0 \quad A_2 = 0.0 \quad K_s = 0.02 \\
V_{ST\mathrm{MIN}} &= -0.1 \quad V_{ST\mathrm{MAX}} = 0.1.
\end{aligned}$$

All resistances and reactances are in *per unit* and time constants in seconds.

Acknowledgment

The authors greatly appreciate the help provided by A. Eichmann, ABB Industrie AG, Turgi, Switzerland, relating to the working of ABB programmable logic controller.

The first author would also like to thank the Faculty of Graduate Studies, University of Calgary, for supporting his Ph.D. work in the form of Izaak Walton Killam Memorial Scholarship.

References

[1] P. Kundur, D. C. Lee, and H. M. Z. El-Din, "Power system stabilizers for thermal units: Analytical techniques and on-site validation," *IEEE Trans. Power App. Syst.*, vol. PAS-100, pp. 81–95, Jan. 1981.

[2] E. V. Larsen and D. A. Swann, "Applying power system stabilizers, Part I-III," *IEEE Trans. Power App. Syst.*, vol. PAS-100, pp. 3017–3046, June 1981.

[3] D. A. Pierre, "A prespective on adaptive control of power systems," *IEEE Trans. Power Syst.*, vol. PWRS-2, pp. 387–396, Sept. 1987.

[4] K. J.Åström and B. Wittenmark, *Adaptive Control*. Reading, MA: Addison-Wesley, 1995.

[5] S. J. Cheng, Y. S. Chow, O. P. Malik, and G. S. Hope, "An adaptive synchronous machine stabilizer," *IEEE Trans. Power Syst.*, vol. PWRS-1, pp. 101–109, Feb. 1986.

[6] A. Ghosh, G. Ledwich, O. P. Malik, and G. S. Hope, "Power system stabilizer based on adaptive control techniques," *IEEE Trans. Power App. Syst.*, vol. PAS-103, pp. 1983–1986, Aug. 1984.

[7] J. W. Finch, K. J. Zachariah, and M. Farsi, "Self-tuning control applied to turbogenerator AVRs," *Proc. Inst. Elect. Eng., Gen., Transm. Distrib.*, vol. 2, no. 3, pp. 492–498, June 1996.
[8] *IEEE Tutorial Course on Artificial Neural Networks with Applications to Power Systems*, M. A. El-Sharkawi and D. Niebur, Eds., The Institute of Electrical and Electronics Engineers, Inc., Piscataway, NJ, 1996.
[9] Q. H. Wu, B. W. Hogg, and G. W. Irwin, "A neural network regulator for turbogenerators," *IEEE Trans. Neural Networks*, vol. 3, pp. 95–100, Jan. 1992.
[10] S. Weerasooriya and M. A. El-Sharkawi, "Laboratory implementation of a neural network trajectory controller for a DC motor," *IEEE Trans. Energy Conversion*, vol. 8, pp. 107–113, Mar. 1993.
[11] Y. Zhang, G. P. Chen, O. P. Malik, and G. S. Hope, "An artificial neural network based adaptive power system stabilizer," *IEEE Trans. Energy Conversion*, vol. 8, pp. 71–77, Mar. 1993.
[12] J. He and O. P. Malik, "An adaptive power system stabilizer based on recurrent neural networks," *IEEE Trans. Energy Conversion*, vol. 12, pp. 413–418, Dec. 1997.
[13] S. Haykin, *Neural Networks: A Comprehensive Foundation*. New York: Macmillan, 1994.
[14] G. P. Chen, O. P. Malik, G. S. Hope, Y. H. Qin, and G. Y. Xu, "An adaptive power system stabilizer based on the self-optimizing pole shifting control strategy," *IEEE Trans. Energy Conversion*, vol. EC-8, pp. 639–646, Dec. 1993.
[15] J. Park and I. W. Sandberg, "Universal approximation using radial-basis-function networks," *Neural Comput.*, vol. 3, pp. 246–257, 1991.
[16] T. Poggio and F. Girosi, "Networks for approximation and learning," *Proc. IEEE*, vol. 78, pp. 1481–1497, 1990.
[17] S. Chen, S. A. Billings, and P. M. Grant, "Recursive hybrid algorithm for nonlinear system identification using radial basis function networks," *Int. J. Control*, vol. 55, no. 5, pp. 1051–1070, 1992.
[18] H. Demuth and M. Beale, *Neural Network Toolbox User's Guide*. Natick, MA: The Math Works, Inc., 1998.
[19] P. M. Mills, A. Y. Zomaya, and M. O. Tade, *Neuro-Adaptive Process Control—A Practical Approach*. New York: Wiley, 1996.
[20] B. Adkins and R. G. Harley, *The General Theory of Alternating Current Machines: Applications to Practical Problems*. London, U.K.: Chapman & Hall, 1975.
[21] *IEEE Standard, IEEE Recommended Practice for Excitation Systems for Power System Stability Studies*, 1992.
[22] Y. N. Yu, *Electric Power System Dynamics*. New York: Academic, 1983.
[23] G. Ramakrishna and O. P. Malik, "RBF identifier and predictive controller for multi-machine power system," in *Proc. IEEE Power Eng. Soc., Summer Meeting*, Edmonton, AB, Canada, July 1999, pp. 1231–1235.
[24] G. Ramakrishna, "Beyond gain-type scheduling controllers: New tools of identification and control for adaptive PSS," Ph.D. dissertation, Univ. Calgary, Calgary, AB, Canada, 2000.

G. Ramakrishna (S'88–M'01) graduated in electrical and electronics engineering from National Institute of Technology, Trichy, India (Formerly Regional Engineering College), in 1992 . He received the M.Sc. and Ph.D. degrees in electrical engineering from the University of Calgary, Calgary, AB, Canada, in 1996 and 2000, respectively.

Currently, he is an Assistant Professor at the University of Saskatchewan, Saskatoon, SK, Canada. He was also a Graduate Engineer with Larsen & Toubro Ltd., Madras, India; Junior Research Fellow with the Indian Institute of Technology, Kanpur, India, Research Engineer with the Center of Intelligent Systems, Rourkela, India; Research Scientist with the Alberta Research Council, Calgary, AB, Canada; and Staff Software Engineer with IBM Toronto Lab, Toronto, ON, Canada. His current areas of interest are power system protection, control and monitoring and real-time simulation of power systems.

Dr. Ramakrishna was the recipient of Alberta Research Council Scholarship in 1996–1997, Izaak Walton Killam Memorial Scholarship in 1998–2000, and NSERC Industrial Research Fellowship in 2000.

O. P. Malik (M'66–SM'69–F'87–LF'00) graduated in electrical engineering from Delhi Polytechnic, India, in 1952. He received the Master's degree from the Indian Institute of Technology, Roorkee (previously named, University of Roorkee) in 1962. He received the Ph.D. degree and D.I.C. from the Imperial College, London, U.K, in 1965.

Currently, he is Professor Emeritus with the University of Calgary, Calgary, AB, Canada, where he has been since 1974. He has served the University of Calgary in various administrative capacities including Acting Dean and Associate Dean. He has published many technical papers in various international journals and conferences and has collaborated in research work with teams from Russia, Ukraine, Switzerland, China, and India. Adaptive power system stabilizers using the algorithm based on the self-tuning principle developed by his research group are currently in commercial operation.